Supporting Information

Poly(butylene succinate) reinforced by small amount of grafted nanofibrillated bacterial cellulose: Toughness variability based on nanocomposites preparation method

Hamidah binti Hashim[a], Xiaochao Xia[a] , Hiroshi Kani[b], Shuichiro Seno[b], Feng Li[c], Takuya Isono[c], Takuya Yamamoto[c], Hirofumi Tani[c], Toshifumi Satoh[c,d], and Kenji Tajima[c] *

[a]Graduate School of Chemical Sciences and Engineering, Hokkaido University, Sapporo, 060-8628, Japan

[b]Hokkaido Research Organization, Industrial Research Institute, Sapporo 060-0819, Japan

[c]Faculty of Engineering, Hokkaido University, Sapporo, 060-8628, Japan

[d]ICReDD List-PF, Hokkaido University, N21W10, Kita-ku, Sapporo 001-0021, Japan

E-mail address:

Hamidah binti Hashim: **bintihashim.hamidah.a7@elms.hokudai.ac.jp**; Xiaochao Xia: **xia.x@wustl.edu**; Hiroshi Kani: **kani-hiroshi@hro.or.jp**; Shuichiro Seno: **seno-shuuichirou@hro.or.jp**; Feng Li: **feng.li@eng.hokudai.ac.jp**; Takuya Isono: **isono.t@eng.hokudai.ac.jp**; Takuya Yamamoto: **yamamoto.t@hokudai.ac.jp**; Hirofumi Tani: **tani@eng.hokudai.ac.jp**; Toshifumi Satoh: **satoh@eng.hokudai.ac.jp**

* Corresponding author: Kenji Tajima

Tel.: +81(11)-706-6567; fax: +81(11)-706-6567

Email address: ktajima@eng.hokudai.ac.jp

Faculty of Engineering, Hokkaido University, N13W8, Kita-ku, Sapporo 060-8628, Japan

Number of pages: 12

Number of figures: 14

Number of tables: 3

Number of equations: 5

1. Materials

Never-dried nanofibrillated bacterial cellulose produced using hydroxypropylcellulose (HPC) (HP-NFBC) (HPC content = 17.4 wt.%, Molar substitution of HPC = 2.95, Molar degree of hydroxypropyl oxide substitution = 0.486) was supplied by Kusano Sakko Inc. HP-NFBC was prepared according to the literature[1]. SA (>95.0%), BO (>99.0%), 1,3,5-trimethoxybenzene (>97.0%), and cesium pivalate (>97.0%) were purchased from Tokyo Chemical Industry Co. Ltd. (Tokyo, Japan). Cesium pivalate was dried at 100 °C under vacuum for at least 72 h prior to use. Methanol (>99%), *n*-hexane (>95.0%), chloroform-*d* ($CDCl_3$, >99.8%), and dichloromethane (CH_2Cl_2, >99.0%) were purchased from Kanto Chemical Co., Inc. (Tokyo, Japan) and used without further purification. Chloroform ($CHCl_3$, >99.0%) was purchased from Junsei Chemical Co. Ltd. (Tokyo, Japan). HP-NFBC (1% dispersion; HPC content: 25 wt%), supplied by Kusano Sakko, Inc. (Ebetsu, Japan), were washed with Milli-Q water and centrifuged (9000 rpm, 15 min, 25 °C) thrice. After freezing at –80 °C for 2 h, the purified HP-NFBCs were lyophilized for 48 h. Prior to grafting, the HP-NFBCs were dried in an oven at 105 °C for 3 h to remove the remaining water molecules.

2. Experimental

2.1 Structural analyses of HPNFBC-*g*-P(SA-*alt*-BO)/PBSs

2.1.1. Fourier-transform infrared spectroscopy

Fourier-transform infrared (FTIR) spectra were recorded on a Perkin Elmer Frontier MIR/UATR instrument in attenuated total reflectance (ATR) mode at a running scan and resolution of 8 and 1 cm^{-1}, respectively. The spectra were normalized in the region from 1723

to 1722 cm^{-1} corresponding to the C=O absorption shown by the carbonyl group belonging to HPNFBC-*g*-P(SA-*alt*-BO). The HP-NFBC spectra were not normalized.

2.1.2. Size extrusion chromatography measurements

The number-average molecular weight ($M_{n,SEC}$) and dispersity ($Đ$) were determined by size extrusion chromatography (SEC) in THF (1.0 mL min^{-1}) using high-performance chromatography equipped with Shodex KF-G guard column, Shodex KF-804L column and RI detector. The SEC apparatus was calibrated using linear polystyrene standards [2].

2.1.3. ^{1}H NMR spectroscopy

Proton nuclear magnetic resonance (^{1}H NMR) spectra were recorded on a JEOL JNM-ECS400 (400 MHz) instrument at 25 °C using $CDCl_3$ as the solvent [internal standard: tetramethylsilane (TMS) (0.00 ppm); number of scans: 8].

2.1.4. Solid-state ^{13}C NMR spectroscopy

Solid-state cross-polarization magic-angle spinning ^{13}C NMR (^{13}C CP/MAS NMR) spectra were obtained using a DSX 300 spectrometer (Bruker, Germany) operating at 75.48 MHz. The samples were packed in a 4.0 mm rotor and spun at a frequency of 4 kHz at contact and recycle times of 1.0 ms and 4 s, respectively. The spectra were calibrated using the carbonyl carbon of glycine (chemical shift: 176.03 ppm) as standard [3].

2.1.5. Atomic force microscopy studies

Atomic force microscopy (AFM) images were obtained using a Hitachi AFM5000II instrument in tapping mode with a silicon cantilever (SI-DF3P2, SII Nanotechnology Inc.) with a resonant frequency and spring constant of 70 kHz and 2.1 N m^{-1}, respectively. The thin films for the AFM studies were prepared by dispersing the respective materials in toluene [0.05

(w/v)%], followed by depositing 5 μL of each dispersion on the surface of a silicon substrate. The films were dried at 30 °C in a drying oven prior to observation.

2.2. Characterization of HPNFBC-*g*-P(SA-*alt*-BO)/PBS nanocomposites

2.2.1. Thermogravimetric analysis

In thermogravimetric analysis (TGA), the decomposition behavior of the samples was studied using a Hitachi STA200RV instrument. The samples (~5 mg) were heated from 25 to 600 °C at a heating rate of 10 °C min^{-1} in a nitrogen-based atmosphere.

2.2.2. Differential Scanning Calorimetry

In differential scanning calorimetry (DSC), the melting points were evaluated using a Hitachi DSC 7000X instrument. The samples (~5 mg) were placed in aluminum pans and sealed hermetically. First, the samples were heated to 150 °C. They were subsequently cooled to –20 °C, and reheated to 150 °C. The cooling and heating rates were 20 and 10 °C min^{-1}, respectively. The experiments were performed in a nitrogen-based atmosphere. The crystallinity, χ_c, of each sample was calculated according to the following equation (eq. 1):

$$\chi_c = \Delta H_m / (w \times \Delta H^o_{100}), \qquad \textbf{(Equation S1)}$$

where ΔH_m is the heat of fusion of the sample, w is the weight fraction of PBS, and ΔH^o_{100} is the heat of fusion of 100% crystalline PBS, 200 J g^{-1}[4].

2.2.3. Polarized optical microscopy

In polarized optical microscopy (POM), micrographs were obtained using an Olympus optical microscope equipped with a Mettler-Toledo hot stage to observe the dispersibility of

HP-NFBC in the nanocomposites. The samples were first place on glass slides, heated from 30 to 150 ℃ at heating rate of 20 ℃ min^{-1}, and then kept at 150 ℃ for 5 min for observations.

2.2.4. Tensile tests.

Dumbbell-shaped film specimens with gauge lengths and widths of 12 and 2 mm, respectively, were prepared for tensile testing. Tensile tests were performed using an INSTRON 34SC-1 tensile tester at a crosshead speed of 10 mm min^{-1} under ambient conditions. The measurements for each film type were repeated 3–5 times and reported as the mean value and standard deviation.

2.2.5. Three-point bending tests.

Three-point bending tests were performed using an Autograph AG-100kNXplus universal testing machine (Shimadzu Corp.). The samples were cut to 80 mm × 10 mm × 2 mm. The span was 32 mm, and the crosshead speed was set to 1 mm/min.

2.3. Structural analyses and characterization of HP-NFBC

Determined according to the literature[1].

2.3.1 Fiber length analysis

All image-processing methods used in this study were performed by importing the AFM file image data as a TIFF image into FiberApp with MATLAB Compiler Runtime 8.1 (MCR), an open-source software for tracking and analyzing fibrous objects [5,6]. The fiber length of each NFBC was acquired from four AFM images with 90 × 90 μm and 1,024 × 1,024 pixels. Overall, data from 544 HP-NFBC fibrils were extracted. The extracted fiber length distribution was extrapolated using the lognormal distribution in eq. S2 and fitted using the least-squares method.

$$f(L_i;\ \mu,\sigma) = \frac{A}{\sqrt{2\pi}\sigma L_i} exp\{-\frac{(logL_i-\mu)^2}{2\sigma^2}\}, \quad \textbf{(Equation S2)}$$

where L_i is the total contour length of the fibrils, μ and σ are the mean value and the standard distribution of the length's natural logarithm, respectively, and A is a distribution normalizing constant. The length-weighted average fiber length L_l is expressed in eq. S3.

$$L_l = \frac{\sum L_i^2 \cdot f(L_i)}{\sum L_i \cdot f(L_i)} \quad \textbf{(Equation S3)}$$

2.3.2 Fiber diameter analysis

The fiber diameter of HP-NFBC was acquired from AFM images with spatial dimensions of 5 × 5 μm and 1,024 × 1,024 pixels. Data was extracted from 842 points from HP-NFBC. The extracted fiber diameter distribution was extrapolated using the normal distribution in eq. S4 and fitted using the least-squares method.

$$f(H_i;\ \mu,\sigma) = \frac{A}{\sqrt{2\pi}\sigma} exp\{-\frac{(H_i-\mu)^2}{2\sigma^2}\}, \quad \textbf{(Equation S4)}$$

where H_i is the total diameter of the fibrils, μ and σ are the mean value and the standard distribution of the diameter, respectively, and A is a distribution normalizing constant. μ is equivalent to the average fiber diameter H.

2.3.3 Degree of oxypropylation of initial HP-NFBC

No. of moles of pyranose ring in HP-NFBC

HP-NFBC = 17.4 wt.% HPC+ 82.6 wt.% cellulose
HP-NFBC$_{100g}$= 17.4 g HPC+ 82.6 g cellulose
Molecular weight of pyranose rings in HPC (Molar substitution (MS) =2.95), $M_{w\_HPC(2.95)}$ = 333.1 g/mol,
Molecular weight of 1 unit cellulose, $M_{w\_cellulose}$ = 162.14 g/mol

$$\text{HPC} = \frac{17.4\ \text{g}}{331.1\ \text{g/mol}} = 0.052\ \text{moles}$$

$$\text{Cellulose} = \frac{82.6\ \text{g}}{162.14\ \text{g/mol}} = 0.510\ \text{moles}$$

$$\text{Total moles} = 0.052 + 0.510 = 0.562\ \text{moles}$$

Degree of oxypropylation relative to the total pyranose rings

$$= \frac{\text{HPC mol}}{\text{Total moles}} \text{ x MS} = \frac{0.052}{0.562} \text{ x } 2.95 = 0.273$$

Degree of oxypropylation per mole of pyranose ring

$$= \frac{\text{Degree of oxypropylation relative to the total pyranose rings}}{\text{Total moles}} = \frac{0.273}{0.562} = \underline{0.486}$$

2.4. Preparation of HPNFBC-*g*-P(SA-*alt*-BO)/PBS nanocomposites' compositions.

The HP-NFBC content was calculated based on the HP-NFBC and P(SA-*alt*-BO) ratios obtained via solid-state ^{13}C CP/MAS NMR spectroscopy to prepare nanocomposites with 5, 2, 0.5, and 0.25 wt% of cellulose. The proportions of PBS and HPNFBC-*g*-P(SA-*alt*-BO) used to prepare the blends were calculated according to the literature[1].

3. Confirmation of polymerization reaction

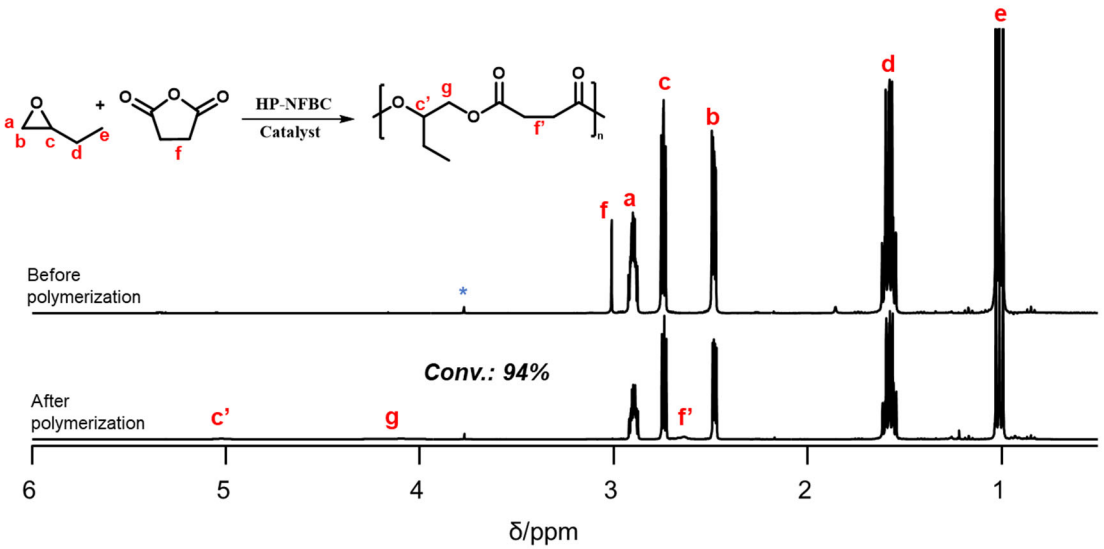

Figure S1 ^{1}H NMR spectra of HPNFBC-*g*-P(SA-*alt*-BO) (33k) before polymerization (upper) and quench of polymerization (lower) (spectra were recorded in $CDCl_3$, operating frequency: 400 MHz). (*internal standard: 1,3,5-trimethoxy benzene).

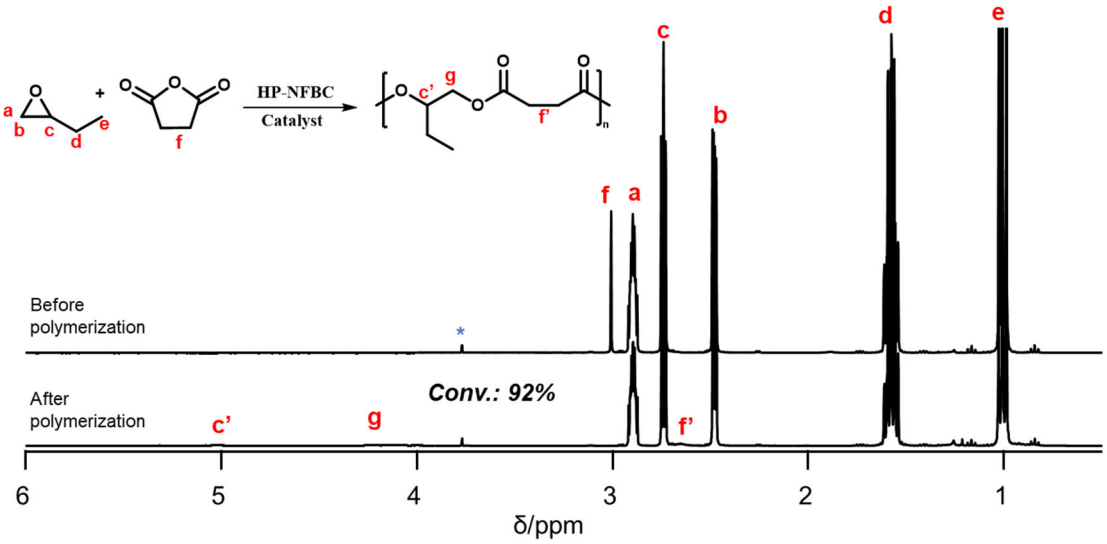

Figure S2 ^{1}H NMR spectra of HPNFBC-*g*-P(SA-*alt*-BO) (29k) before polymerization (upper) and quench of polymerization (lower) (spectra were recorded in $CDCl_3$, operating frequency: 400 MHz). (*internal standard: 1,3,5-trimethoxy benzene).

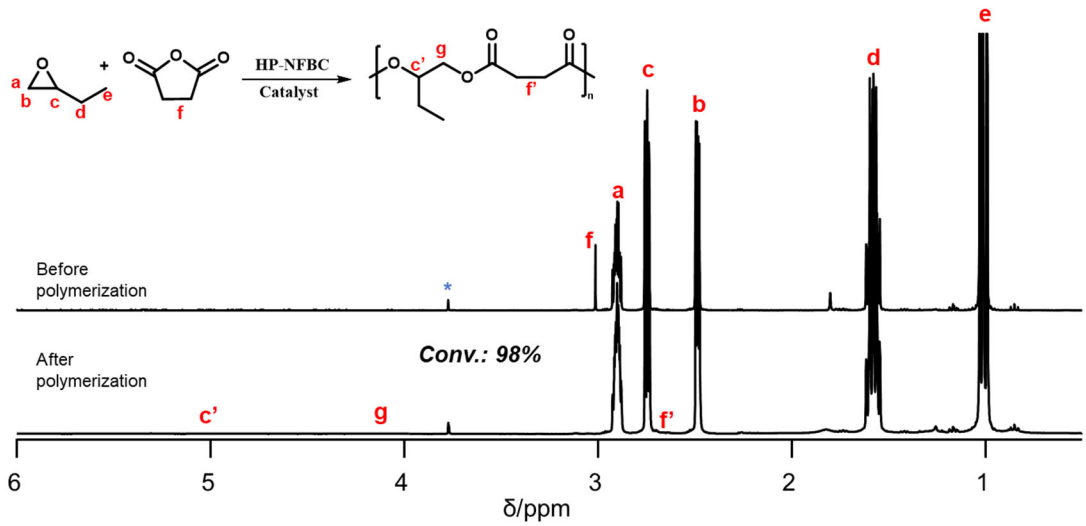

Figure S3 ^{1}H NMR spectra of HPNFBC-*g*-P(SA-*alt*-BO) (15k) before polymerization (upper) and quench of polymerization (lower) (spectra were recorded in $CDCl_3$, operating frequency: 400 MHz). (*internal standard: 1,3,5-trimethoxy benzene).

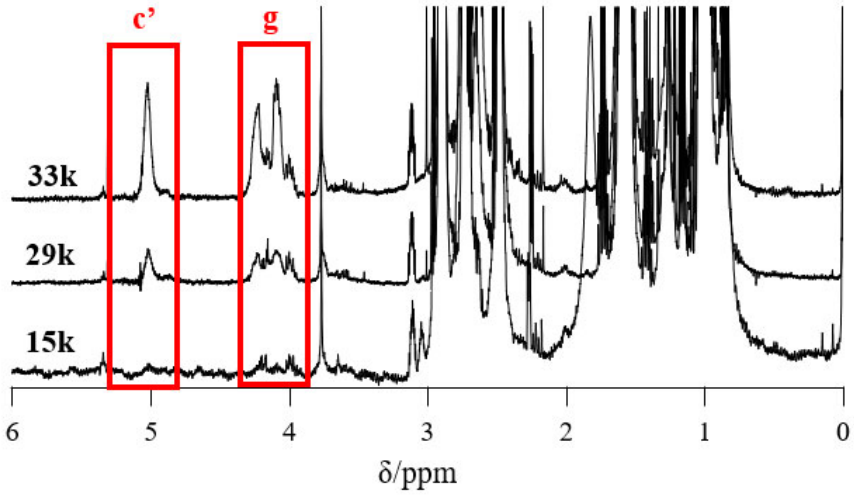

Figure S4 The c' and g peak of alternating P(SA-*alt*-BO) in each sample.

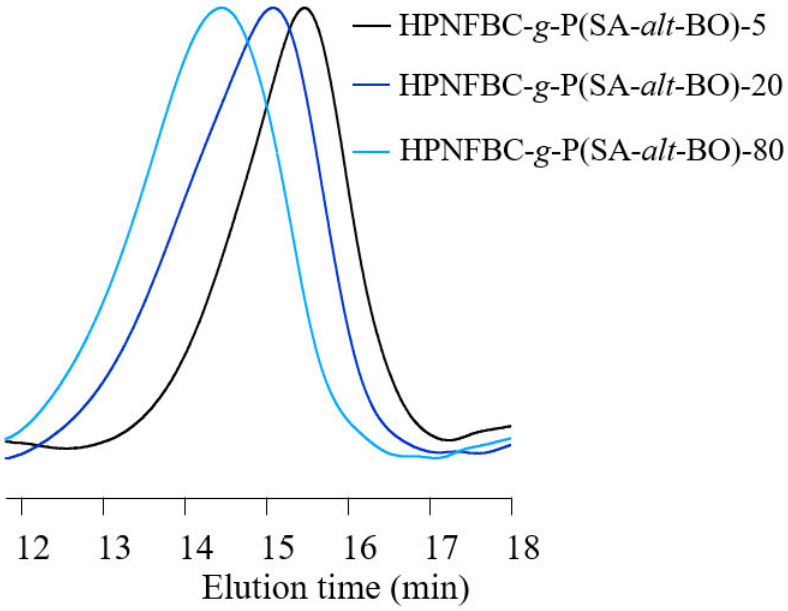

Figure S5 Size-exclusion chromatography (SEC) traces of HPNFBC-*g*-P(SA-*alt*-BO)s (eluent, THF; flow rate, 1.0 mL min−1; Polystyrene standard)

Table S1 Compositions of P(SA-*alt*-BO)s and HP-NFBC[a].

Sample	Compositions (mol %)			
	SA	**BO**	**P(SA-*alt*-BO)**	**HP-NFBC**
HPNFBC-*g*-P(SA-*alt*-BO) (33k)	40.3	47.9	88.2	12.1
HPNFBC-*g*-P(SA-*alt*-BO) (29k)	38.8	33.6	72.4	27.6
HPNFBC-*g*-P(SA-*alt*-BO) (15k)	31.6	26.7	58.3	41.7

[a]Determined by CP/MAS ^{13}C NMR relaxation experiment.

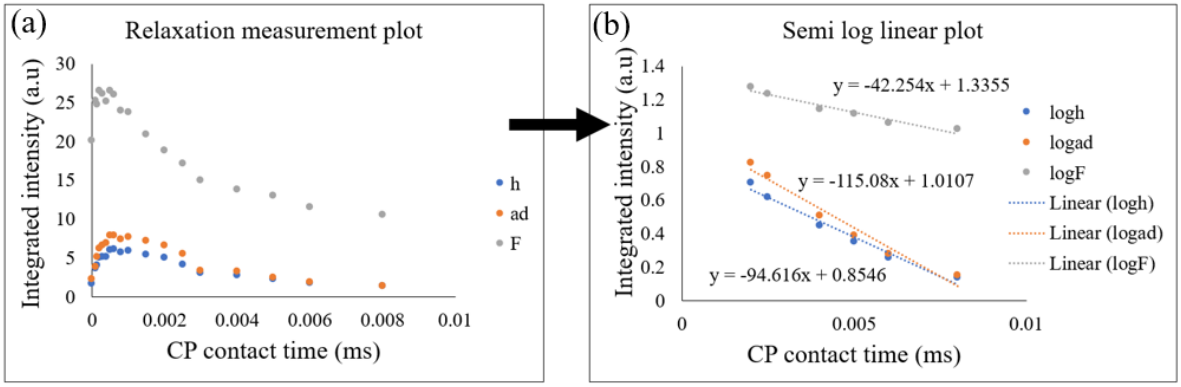

Figure S6. (a) Cross polarization (CP) time-relative magnetization graph obtained through nuclear magnetic resonance (NMR) relaxation time experiment **(b)** linear approximation of semi-log of points.

Equation S5:

$$\text{Coefficient} = \frac{\text{y-intersection (}\textbf{Figure S5(b)}\text{)}}{\text{integral value of each respective peak from relaxation measurement sample}}$$

4. Morphological properties of HPNFBC-*g*-P(SA-*alt*-BO)

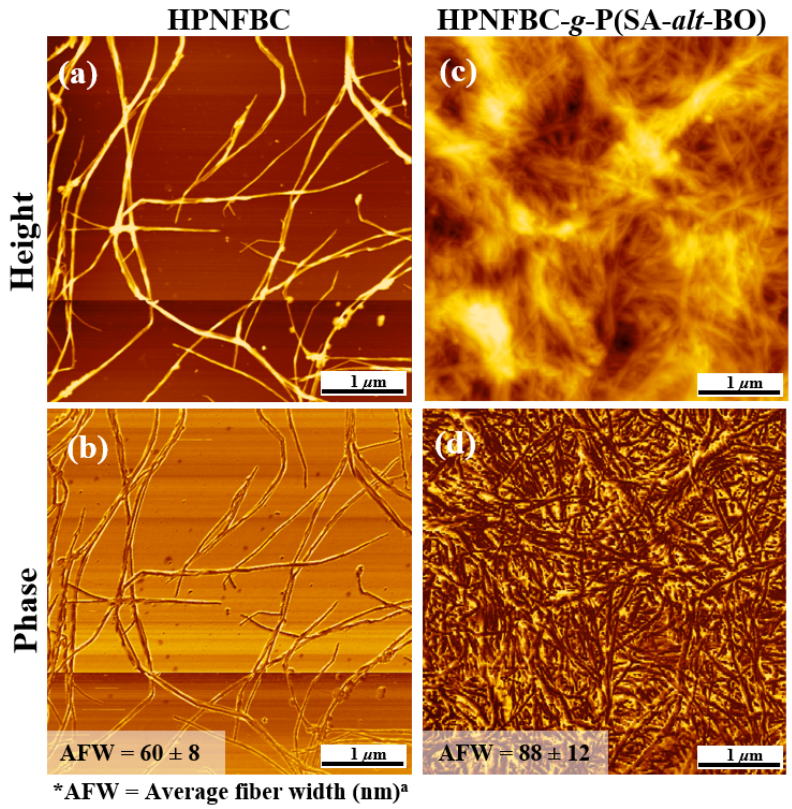

[a]calculated by Image J software from average value of 50 samples.

Figure S7 Atomic force microscopy (AFM) images of HPNFBC-g-P(SA-alt-BO) showing higher average fiber width compared to HP-NFBC

5. Mechanical properties of HPNFBC-*g*-P(SA-*alt*-BO)/PBS nanocomposites.

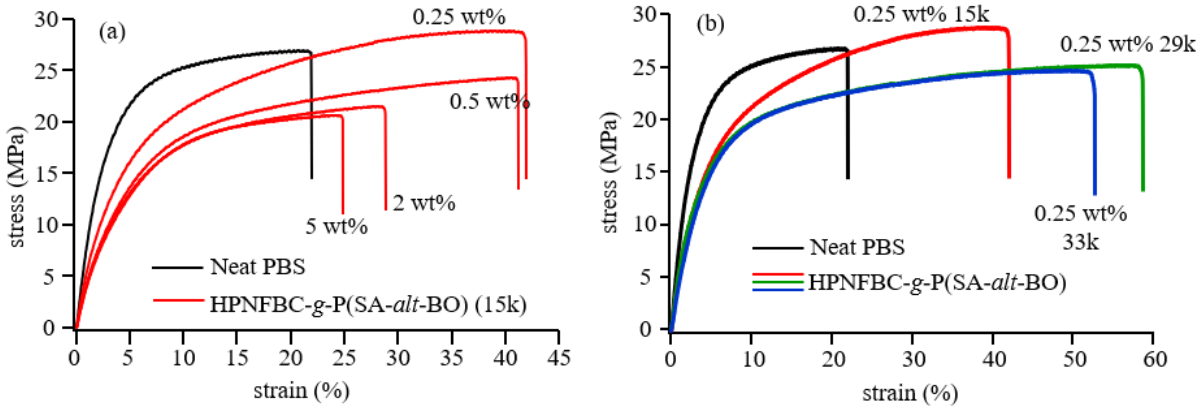

Figure S8 Stress-strain curves of polybutylene succinate (PBS) and PBS nanocomposites by varied compositions percentage **(a)** and varied copolymer chain length **(b).**

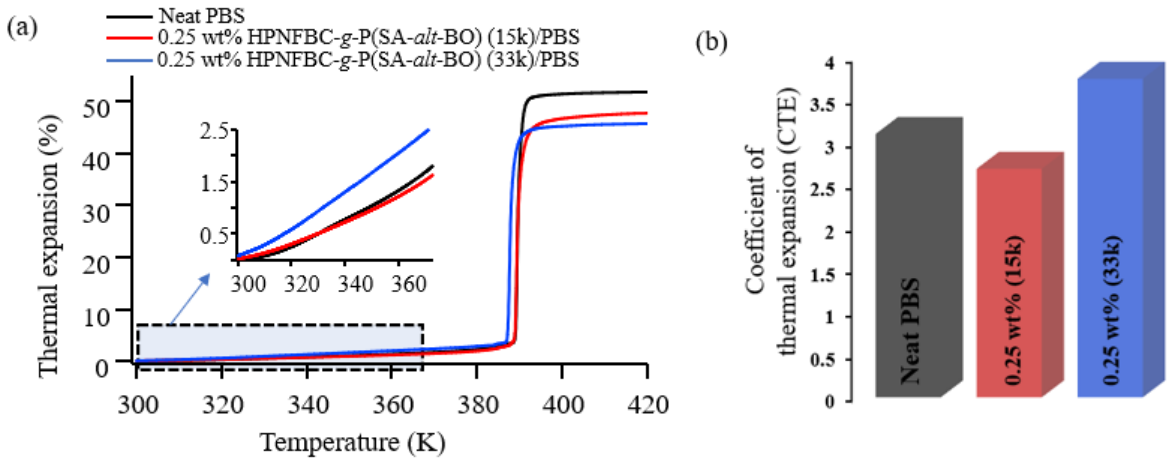

Figure S9 (a) Thermomechanical analysis (TMA) curves of HPNFBC-*g*-P(SA-*alt*-BO)/PBS of long and short grafted copolymer chain length and comparison with pure PBS. **(b)** Coefficient of nanocomposites thermal expansions (60–100°C).

6. Thermal properties of nanocomposites

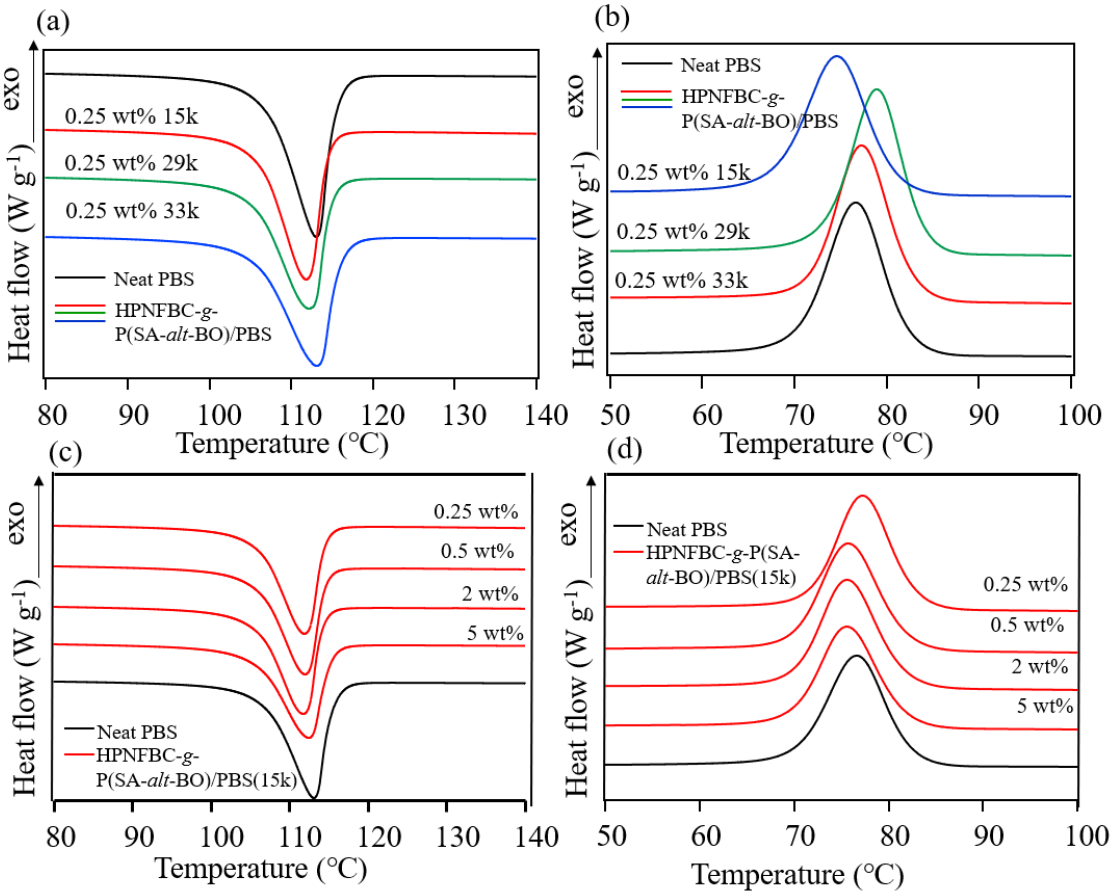

Figure S10 (a) 1st heating (b) 1st cooling thermograms of nanocomposites with different length and **(c)** 1st heating (d) 1st cooling differential scanning calorimetry (DSC) thermograms of nanocomposites with different compositions wt%. Each thermogram were compared with pure PBS (M_w 44700; *Đ,* 2.2).

Table S2 Characterization of thermal properties of HPNFBC-*g*-P(SA-alt-BO)/PBSs, pure PBS, and HP-NFBC.

Sample	HPNFBC-*g*-P(SA-*alt*-BO)-5 composition (wt.%)	T_m (°C)	ΔH_m (J/g)	T_c (°C)	ΔH_c (J/g)	χ_c (%)
HPNFBC-*g*-P(SA-*alt*-BO)(15k)/PBS	5	112.5	85.5	75.9	58.8	45.0
	2	111.8	93.2	75.8	62.0	47.6
	0.5	112.0	91.6	75.7	62.9	46.0
	0.25	111.9	85.1	77.7	63.5	42.7
HPNFBC-*g*-P(SA-*alt*-BO)(29k)/PBS	0.25	112.2	91.4	79.4	62.4	45.8
HPNFBC-*g*-P(SA-*alt*-BO)(33k)/PBS	0.25	113.1	102	74.2	66.2	51.1
Neat PBS	0	113.1	101	76.7	66.8	50.5

[a]Temperature at which sample start losing weight.; [b]Maximum weight loss temperature

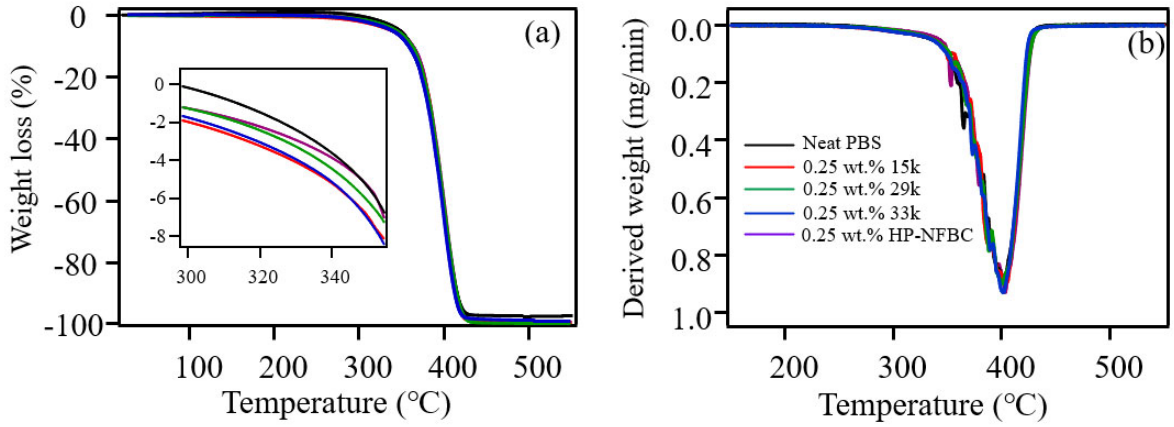

Figure S11 (a) Thermogravimetry (TG) and **(b)** differential thermal gravity (DTG) curves of HP-NFBC, HPNFBC-*g*-P(SA-*alt*-BO)/PBS and PBS (Mw 44700).

Table S3 Thermal stability of the PBS nanocomposites analyzed by TGA.

Sample	$T_{onset}(T_{5\%})^a$ **(°C)**	$T_{max}{}^b$ **(°C)**
Neat PBS	348.2	401.8
0.25 wt% HPNFBC-*g*-P(SA-*alt*-BO)(29k)/PBS	338.3	405.1
0.25 wt% HPNFBC-*g*-P(SA-*alt*-BO)(33k)/PBS	343.7	401.5
0.25 wt% HPNFBC-*g*-P(SA-*alt*-BO)(15k)/PBS	339.1	401.8
0.25 wt% HP-NFBC/PBS	348.0	403.6

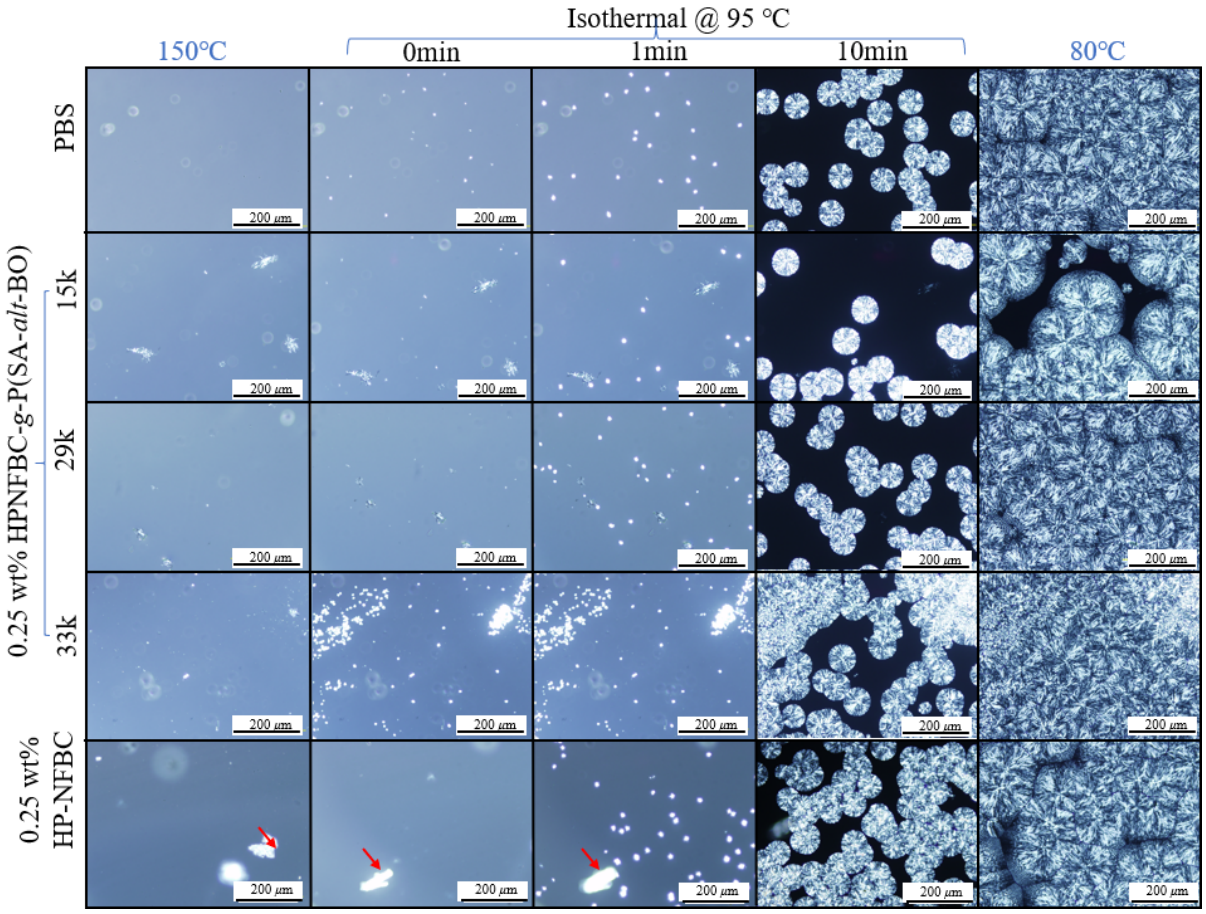

Figure S12 Polarized optical microscopy (POM) images of each type of nanocomposites in comparison with the pure PBS.

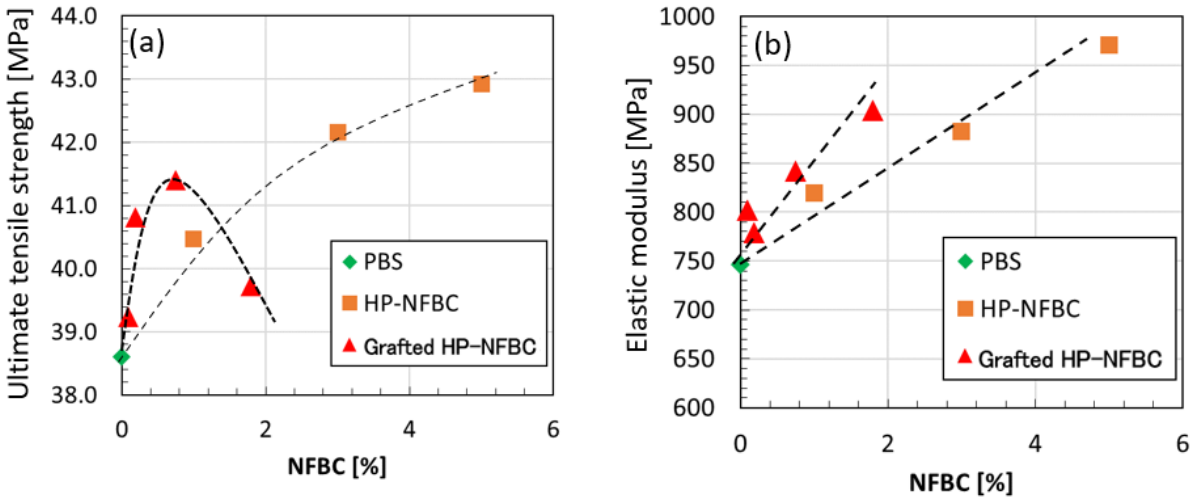

Figure S13 Mechanical properties by flexural tests of nanocomposites prepared by melt-kneading process. **(a)** Ultimate flexural strength, **(b)** elastic modulus.

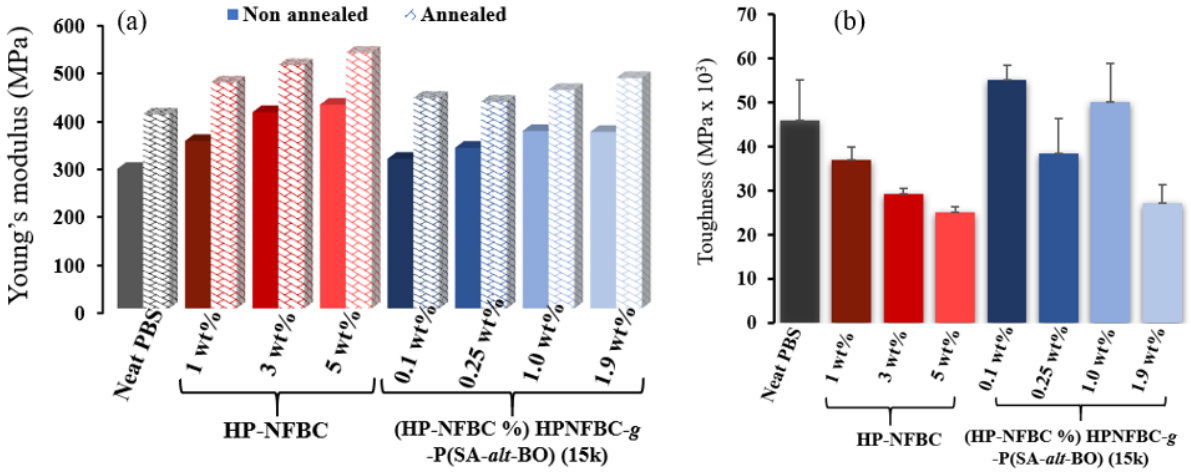

Figure S14 (a) Enhanced Young's modulus after thermal annealing. (b) Toughness comparison of each nanocomposites compared to neat PBS.

References

[1] Hashim H binti, Emran NAA binti, Isono T, Katsuhara S, Ninoyu H, Matsushima T, et al. Improving the mechanical properties of polycaprolactone using functionalized nanofibrillated bacterial cellulose with high dispersibility and long fiber length as a reinforcement material. Compos Part A Appl Sci Manuf 2022;158:106978. https://doi.org/10.1016/j.compositesa.2022.106978.

[2] Katsuhara S, Takagi Y, Sunagawa N, Igarashi K, Yamamoto T, Tajima K, et al. Enhanced Self-Assembly and Mechanical Properties of Cellulose-Based Triblock Copolymers: Comparisons with Amylose-Based Triblock Copolymers. ACS Sustainable Chemistry and Engineering 2021;9:9779–88. https://doi.org/10.1021/acssuschemeng.1c02180.

[3] Nomura S, Kugo Y, Erata T. 13C NMR and XRD studies on the enhancement of cellulose II crystallinity with low concentration NaOH post-treatments. Cellulose 2020;27:3553–63. https://doi.org/10.1007/s10570-020-03036-6.

[4] Ma P, Cai X, Wang W, Duan F, Shi D, Lemstra PJ. Crystallization behavior of partially crosslinked poly(β- hydroxyalkonates)/poly(butylene succinate) blends. Journal of Applied Polymer Science 2014;131:1–8. https://doi.org/10.1002/app.41020.

[5] Usov I, Mezzenga R. FiberApp: An open-source software for tracking and analyzing polymers, filaments, biomacromolecules, and fibrous objects. Macromolecules 2015;48:1269–80. https://doi.org/10.1021/ma502264c.

[6] Usov I, Nyström G, Adamcik J, Handschin S, Schütz C, Fall A, et al. Understanding nanocellulose chirality and structure-properties relationship at the single fibril level. Nat Commun 2015;6. https://doi.org/10.1038/ncomms8564.